

DETUNING CURVE ANALYSIS ON THE UVSOR2 FREE ELECTRON LASER

M. Labat, M.E. Couprie, CEA, Saclay, France
Y. Takashima, University of Nagoya, Nagoya, Japan
M. Hosaka, A. Mochihashi, M. Katoh, IMS, Okasaki, Japan

Abstract

Storage Ring Free Electron Laser (FEL) dynamics and behaviour can be explored versus the detuning, i.e. a small difference between the frequencies of revolution of the electron bunches, and of the optical pulse circulating into the optical cavity. In fact, it provides situations ranging from the maximum initial gain over losses conditions to threshold ones. A complete detuning curve gives the intensity of the FEL versus the detuning. Streak camera provides a full characterisation of the FEL versus detuning: position of the centre of mass of the laser, bunch lengthening. The energy spread is deduced from the electron beam transverse sizes. The analysis of the FEL behaviour versus detuning is compared with simulations performed with LAS. The detuning behaviour is then illustrated under different cases.

INTRODUCTION

Systematic measurements of the detuning curves have already been performed on super-ACO [1] and ELETTRA [2] storage rings, and are presented here for UVSOR2 [3] which main characteristics are presented in Table 1.

Table 1: UVSOR2 Storage Ring characteristics

Parameter	Value
Circumference	53.2 m
Energy	600 MeV
Number of bunches	1 or 2
Momentum Compression Factor	0.026
Period of revolution	177 ns
Synchrotron frequency	12656 Hz
Natural energy spread	0.00034
Filling factor	0.872
Order of interference in klystron	87.5
Radius of curvature of magnets	2.2 m

In a Storage Ring Free Electron Laser, the amplification process results from the interaction between the relativistic electron bunches and the electromagnetic wave. The beam-beam interaction occurs at each pass of the electron bunch within the undulator, imposing a pulsed temporal structure to the FEL which will therefore depend on the storage ring used. In the case of UVSOR2, the laser is pulsed at 5.65 MHz, the bunches being spaced

out by 177 ns. This pass by pass interaction requires a synchronization, the so-called Detuning, between the frequency of revolution of the electrons, given by the RF cavity frequency, and the frequency of the laser pulse oscillations inside the optical cavity. Any variation of the detuning introduces delay between the two beams, leading to un-optimized overlapping at each pass, resulting into a pulsed structure at ms scale. Both structures can be analysed with a double sweep Streak Camera, as illustrated in Figure 1.

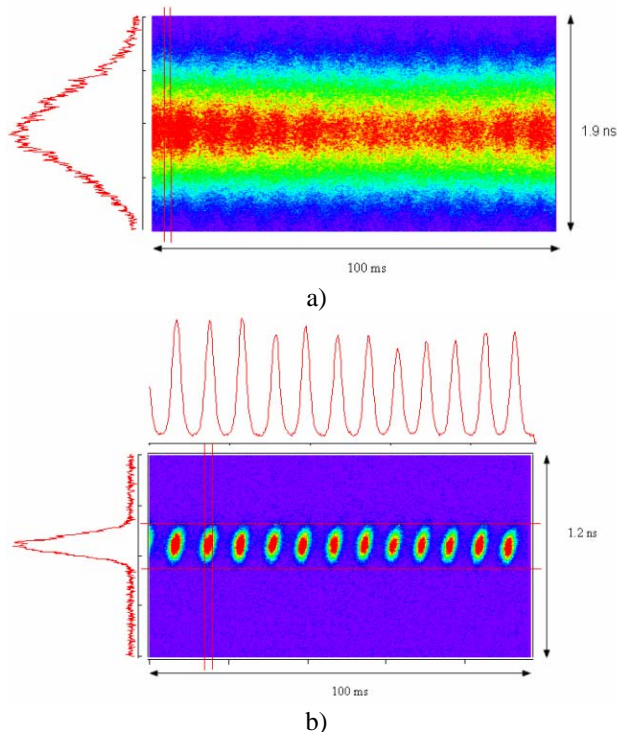


Figure 1: Images obtained with Streak camera (Hamamatsu, C5680) on UVSOR2 FEL, I=12 mA. a) Electron beam, b) Laser beam in pulsed mode of emission. The vertical profile enables to study the temporal lengths of the beams, whereas the horizontal one shows their evolution in time.

EXPERIMENTAL DETUNING CURVES

Around perfect tuning, the intensity of the laser is continuous (cw). For higher values of the detuning, the intensity varies in order to form macro pulses at frequencies around kHz, as illustrated in Figure 1.b. When increasing the detuning, the laser comes back to a continuous mode of emission, until intensity falls back to

zero. The evolution of the laser behaviour versus detuning is illustrated by the so-called Detuning Curves, which can be visualized both with oscilloscope and Streak Camera as illustrated in Figure 2. On the Figure 2.a, one can clearly distinguish the successive modes, defining five zones. The central zone, corresponding to the continuous mode around perfect tuning, zones 2 and 4 corresponding to pulsed modes, and the edges of the curve with again, a constant intensity. In the case of ELETRA, there is no central zone, whereas in the case of UVSOR2 (and super-ACO) it can reach 10 Hz (see fig. 2.a). The Hopf bifurcations [4], transitions between modes of emission, reveal a change in the non linear dynamical behaviour of the laser.

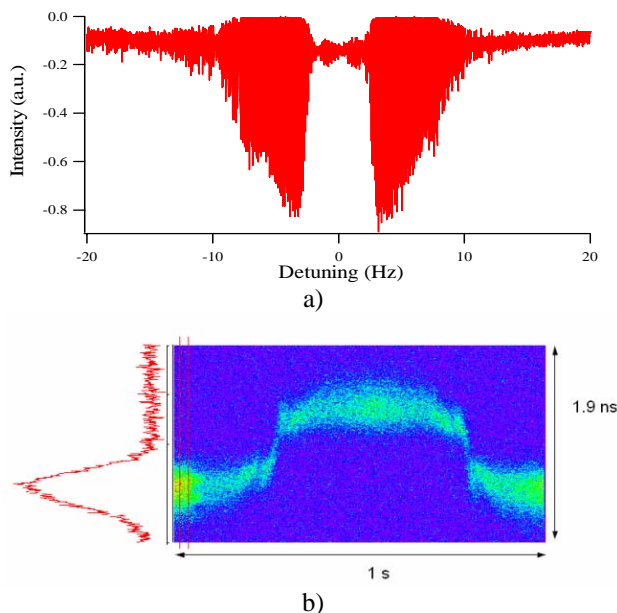


Figure 2: Detuning curve (a ramp is applied with an external frequency generator). $\eta=0$ m, $\lambda=520$ nm, $P=0.13$ %. a) Oscilloscope signal with $I=8.5$ mA, b) Streak Camera image with $I=30$ mA.

The detuning introducing a delay in the synchronization between laser and bunches, the relative position in time of the laser with respect to the electron bunch is modified, as illustrated in Figure 3. The behaviour of this position versus detuning is similar to an arctangent function. The larger is the detuning, the smaller the variation in position.

The spectral width, and the duration of the pulses at micro-temporal scale increase with the detuning, while the power decreases. The temporal interval between two macro pulses is found increasing with detuning, as expected in [5].

FEL INFLUENCE ON THE ELECTRON BEAM

Figure 4 illustrates the electron bunch heating versus the detuning. During the interaction between the two beams, an energy exchange occurs, inducing an energy spread in the electronic distribution. The electron bunch is

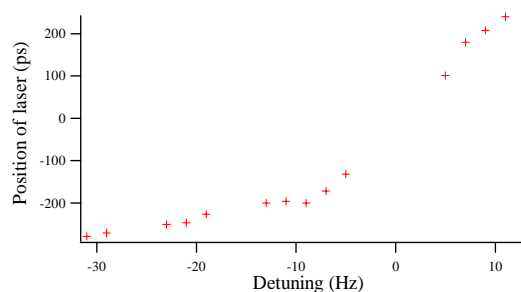


Figure 3: Position of the laser versus detuning. $I=10$ mA, $\eta=0$ m, $\lambda=520$ nm, $P=0.13$ %. Measurement with Streak Camera.

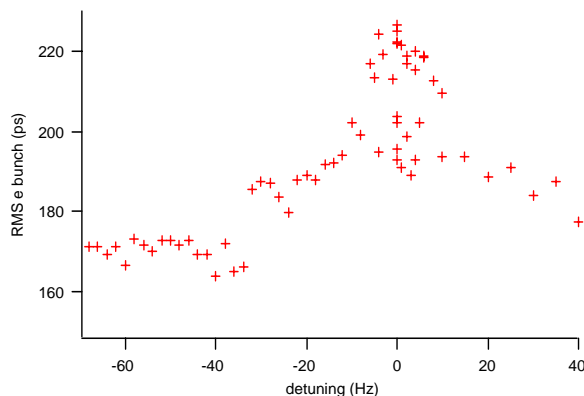


Figure 4: Bunch length versus detuning. $I=10$ mA, $\eta=0$ m, $\lambda=520$ nm, $P=0.13$ %.

heated, and saturation reached for higher values of energy spread. When the detuning is increased, the reduced overlapping between the two beams makes this energy exchange less efficient, and thus the heating of the bunches decreases. Maximum enhancement is found in the central zone, i.e. at perfect tuning.

THEORETICAL MODEL FOR DETUNING ANALYSIS

The longitudinal dynamic of a SRFEL can be described using heuristic equations, describing the coupled evolution of the electromagnetic field and the electron bunch. The LAS code using this description was initially developed by M. Billardon in [6], and already gave satisfactory results on super-ACO [1]. Other approaches rely on the analysis of the amplitude of the electric field [7] of the FEL. In LAS, the three fundamental equations of the laser intensity and gain, and of the energy spread, enable the calculation at each pass of the bunch in the klystron. The laser intensity profile y_n is defined at pass n by:

$$y_n(\tau) = (1 - P)y_{n-1}(\tau)[1 + g_n(\tau)] + i_s \exp\left(-\frac{(\tau+d)^2}{2\sigma_\tau^2}\right),$$

where τ the temporal position with respect to the centre of the electronic distribution, i_s the spontaneous emission, P the cavity losses, σ_τ the rms width of the electron

bunch, and δ the detuning. The gain of the laser, g_n is defined by: $g_n(\tau) = G_0 \left(\frac{P}{G_0}\right)^{\Sigma_n} \exp\left(-\frac{(\tau+\delta)^2}{2\sigma_\tau^2}\right)$, with G_0

the initial peak gain (laser off) [8]. The evolution of the normalised laser-induced energy spread,

$$\Sigma_n = \frac{\sigma_{\gamma n}^2 - \sigma_{\gamma 0}^2}{\sigma_{\gamma e}^2 - \sigma_{\gamma 0}^2}, \quad \text{is given by:}$$

$$\sigma_{\gamma n}^2 = \sigma_{\gamma(n-1)}^2 - \frac{2T_0}{\tau_S} (\sigma_{\gamma(n-1)}^2 - \sigma_{\gamma e}^2) + \frac{2T_0}{\tau_S} (\sigma_{\gamma e}^2 - \sigma_{\gamma 0}^2) I_{n-1}$$

. $\sigma_{\gamma n}$ is the energy spread at n-th pass, $\sigma_{\gamma e}$ its equilibrium value, and $\sigma_{\gamma 0}$ its initial value (laser off). T_0 stands for the revolution period of the bunches, and τ_S for the damping time. The equilibrium of the FEL is assumed to be reached when the cavity losses equal the gain. This leads to the following definition for the equilibrium

$$\text{energy spread: } \sigma_{\gamma e} = \sqrt{\sigma_{\gamma 0}^2 - \frac{\log(P/G_0)}{8(\pi(N+N_D))^2}}.$$

Figure 5 presents the position of the centre of mass and of the maximum of intensity of the laser, and the pulse duration. These values are obtained with LAS code by momenta calculations, whereas the laser power is evaluated with the Renieri limit [9].

Good qualitative agreement is found. The transitions between continuous and pulsed modes appear, and give the same global behaviour for the laser. Differences still remain as far as the width of the curve is concerned, which could be due to averaging if the measurements.

VARIATION OF CONDITIONS

Here is studied the evolution of the detuning curve versus different parameters.

Current

Figure 6 presents the broadening of the detuning curves with current, observed on UVSOR2 FEL. An increase of the current induces via the potential well distortion [10], an enhancement of the bunch length. The temporal interval on which the laser pulse and the electron bunch overlap can be increased, allowing larger values of detuning. In addition, the initial gain increases with the current. The required conditions of equilibrium (gain equal losses) can be satisfied for higher values of detuning, i.e. for less efficient energy exchange.

The central zone is larger as current increases, offering more possibilities in the continuous mode, probably the most useful for potential users.

Dispersion function

The function of dispersion η is fully determined by the optic magnetic functions. The experimental session on the FEL at UVSOR2 allowed to test a new operating point characterised by a non zero dispersion function in the

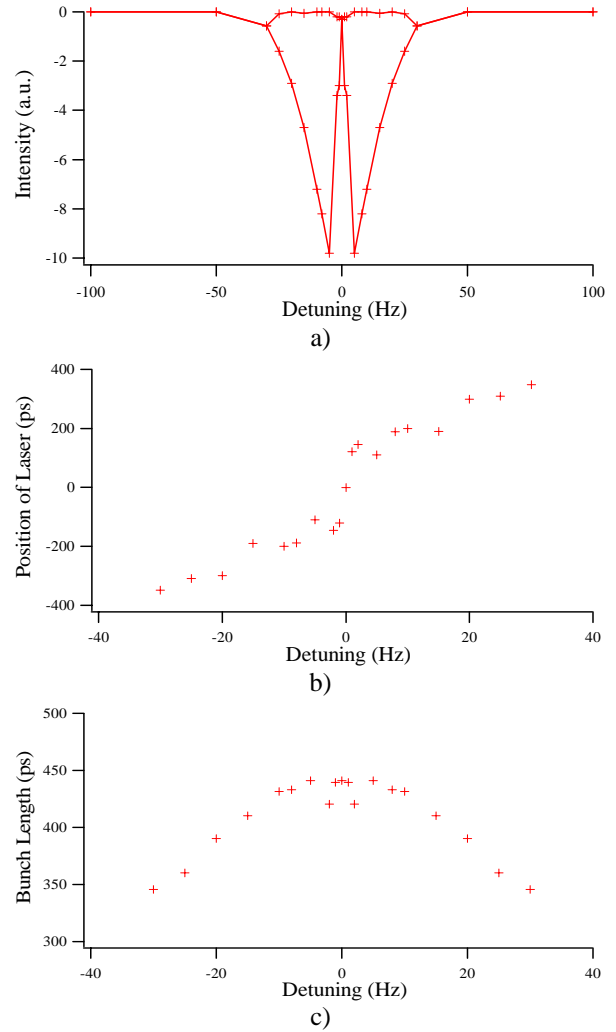


Figure 5: Simulation of detuning with LAS. The parameters used for simulation are those presented in Table 1, with $I=9$ mA, $\eta=0$ m, $P=0.13\%$, $G_0=0.4\%$. a) Detuning curve, b) Position of the laser, c) Bunch length.

optical klystron [11]. Former studies had been lead on SuperAco storage Ring with, in addition, a lower value of the momentum compression factor [12], and had revealed new equilibrium conditions for the FEL. The change from an achromatic to chromatic optics implies modifications in the expression of the transverse dimension of the beam, given by the following relation [13]:

$\sigma_x = \sqrt{\epsilon_x \beta_x + \eta_x^2 \sigma_\gamma^2}$, where ϵ is the emittance of the electron beam, and β the magnetic function. By modifying the transverse dimensions of the beam, one modifies the gain of the laser. Because the transverse dimensions become coupled to the energy spread, these will add their contribution to the gain reduction, and therefore to the saturation process. Equilibrium is reached for smaller values of energy spread. This was experimentally confirmed on UVSOR2 facility. As far as the theoretical model is concerned, the LAS code was modified in order to consider chromatic optics, and led to

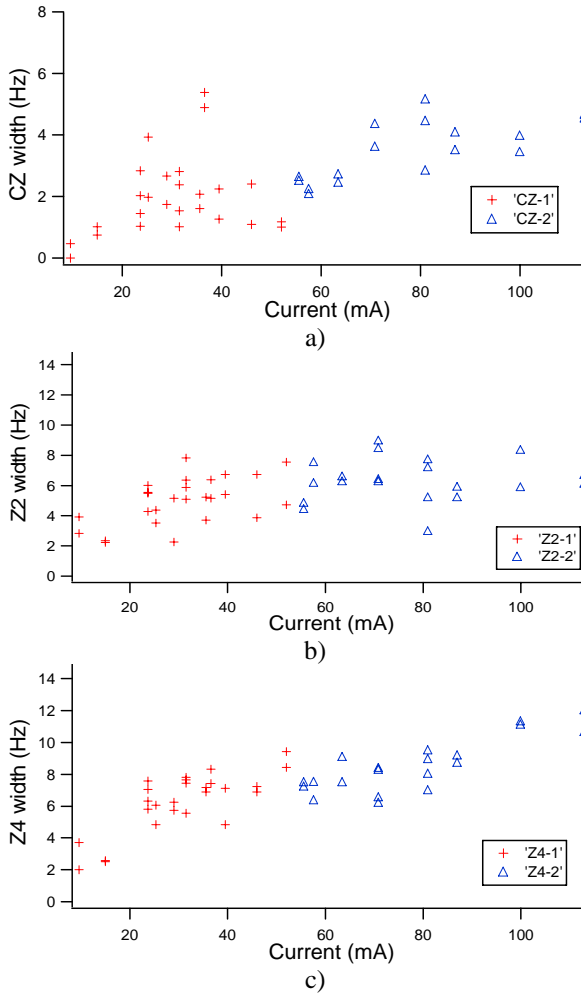


Figure 6: Zones width versus current, a) Central zone, b) First pulsed zone, c) Second pulsed zone. $\eta=0$, $\lambda=520$ nm, $P=0,12$ %.

the same results. In terms of detuning curve, they are theoretically found narrower in the case of chromatic optics, as illustrated in Figure 7. The experiments on UVSOR2 also confirmed this evolution.

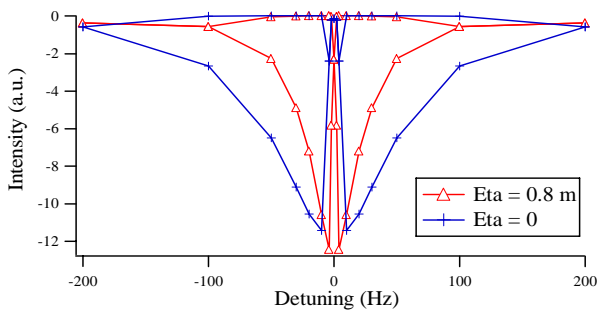


Figure 7: Simulation of detuning with LAS in chromatic ($\eta x=0.8m$) and achromatic ($\eta y=0$) case. The parameters used for simulation are those presented in Table 1, with $I=80$ mA, $P=0.12$ %, $G_0=2.1$ % for $\eta=0$ m, and $G_0=2.7$ % for $\eta=0.8$ m, and $\sigma_{\gamma 0}=0.00044$.

CONCLUSION

The experiments led on UVSOR2 facility enabled to characterize the laser versus detuning, offering various lasing possibilities in terms of temporal structure and beam characteristics. Those various behaviours revealed to be properly described by LAS model. In addition, the detuning with chromatic optics was successfully tested and simulated. This move forward in understanding the FEL dynamic under new magnetic conditions is encouraging, thus modern storage rings, in quest of the smallest emittance for the user's operations [14], tend to use non zero dispersion function.

ACKNOWLEDGMENTS

The author would like to thank S. Bielawski from PHLAM, Université de Lille (France) for his help.

REFERENCES

- [1] C. Bruni, D. Garzella, M.E. Couprie, Proceedings of EPAC, 793-795 (2002).
- [2] G. De Ninno, M. Trov'ò, M. Danailov, M. Marsi, B. Diviacco, Proceedings of the European Particle Accelerator, Conference, Strona 799, 2002.
- [3] M. Katoh, Successful Commissioning of UVSOR-II, Synchrotron Radiation News, 16(6), 2003.
- [4] G. De Ninno, D. Fanelli. "Controlled Hopf Bifurcation in a Storage Ring Free Electron Laser". Phys. Rev. A, 47:3276, 1993.
- [5] D. Fanelli, G. De Ninno, M.E. Couprie, "Detuned dynamics of a Storage Ring Free Electron Laser", Nucl. Inst. Meth. A483 (2002) 177-180.
- [6] M. Billardon, D. Garzella, M.E. Couprie. "Saturation Mechanism for a Storage Ring Free Electron Laser". Phys. Rev. Lett. 92, 094801 (2004).
- [7] S. Bielawski, C. Bruni, D. Garzella, G.-L. Orlandi and M.E. Couprie, Phys. Rev. Lett. to appear.
- [8] P. Elleaume, "The Optical klystron", J. Phys. (Paris) 44, C1-353 (1983).
- [9] A. Renieri, "Storage ring operation of the free electron laser : the amplifier", Il Nuovo Cimento, 50B:160, (1979).
- [10] R.Roux, M.E. Couprie, R.J. Baker, D. Garzella, D. Nutarelli, L. Nahon, M. Billardon, Phys. Rev. E 58 (1998) 6584-6593.
- [11] M. Hosaka, "Storage Ring Free-Electron Laser Saturation for Chromatic and Achromatic Optics", WEOA002, FEL2005.
- [12] G. L. Orlandi, C. Bruni, D. Garzella, and M.E. Couprie, "Super-Aco Electron Beam Dynamics with a Reduced Momentum Compaction Factor Free Electron Laser Operation", 796-798, EPAC 2002.
- [13] M. Sands, "The physics of Electron Storage Rings. An introduction", 373-379, (1971).
- [14] A. Nadji, EPAC, Vienna, Austria, 1057-1059, (2000).